PHYSICS

Theoretical and experimental researches of size effect in micro-indentation test

WEI Yueguang (魏悦广), WANG Xuezheng (王学峥), WU Xiaolei (武晓雷) & BAI Yilong (白以龙)

LNM, Institute of Mechanics, Chinese Academy of Sciences, Beijing 100080, China
Correspondence should be addressed to Wei Yueguang (e-mail: ywei@lnm.imech.ac.cn)

Received April 4, 2000

Abstract Micro-indentation tests at scales on the order of sub-micron have shown that the measured hardness increases strongly with the indent depth or indent size decreasing, which is frequently referred to as the size effect. However, the trend is at odds with the size-independence implied by conventional elastic-plastic theory. In this paper, strain gradient plasticity theory is used to model the size effect for materials undergoing the micro-indenting. Meanwhile, the micro-indentation experiments for single crystal copper and single crystal aluminum are carried out. By the comparison of the theoretical predictions with experimental measurements, the micro-scale parameter of strain gradient plasticity theory is predicted, which is fallen into the region of 0.8—1.5 micron for the conventional metals such as copper (Cu), aluminum (Al) and silver (Ag). Moreover, the phenomena of the pile-up and sink-in near micro-indent boundary are investigated and analyzed in detail.

Keywords: micro-indentation test, size effect, strain gradient plasticity, micro-scale.

Indentation test is an important and effective experimental method, and has been used extensively to estimate the plastic properties of solids undergoing the plastic deformation. Through indentation test, the loading-unloading relation between hardness and depth is measured, by which the material parameters such as the yielding stress, strain hardening exponent, Young's modulus are estimated. Recently, with the enhancement of experimental technique and measure precision, it is possible to carry out the indentation tests at the scale levels of one micron or sub-micron for obtaining more detailed material information. Such small-scale experiments are frequently referred to as micro-indentation tests (or nano-indentation tests). In the micro-indentation test, a new result, which is different from the conventional one, the size-dependent hardness has been revealed extensively[1—8]. For metal materials, the measured hardness may be doubled or even tripled comparing with the conventional hardness as the indent size (or depth) decreases to a fifth micron. However, the trend is at odds with the size-independence implied by conventional elastic-plastic theory. Otherwise, from the dimensional consideration[9], the hardness was only dependent on macroscopic parameters of material, i.e. was size-independence.

In order to predict the size effect phenomena, recently several versions of strain gradient plasticity theories have been presented[10—12]. These theories include the strain gradient effects and have the conventional elastic-plastic theory frame. In the new constitutive relations, the strain components are matched with the new strain gradient components through several length pa-

rameters (or called micro-scales in the following sections). Thus the material size effect can be characterized by the micro-scale parameters.

On the researches of the size effect in the indentaiton tests by using strain gradient plasticity theories, in ref. [4], the case when micro-scale was smaller than the contact radius by adopting the couple stress theory[10] under incompressible assumption was analyzed. In ref. [3], the similar case to ref. [4] but adopting the general theory of the Fleck and Hutchinson's strain gradient plasticity[10] version was analyzed. Furthermore, by applying the prediction result to the micro-indentation test for material tungsten (W)[8], the micro-scale for material W was obtained within 0.25—0.52 micron.

Alternatively, a dislocation model has been used to study the size effect in the micro-indentation test in ref. [1]. By using the Taylor's relation, Mises' plastic flow law and the conventional relation between the hardness and the flow stress, an inverse square root relation between hardness and indent depth was obtained.

By comparing the micro-indentation test results of conventional metals (Cu, Ag, Al)[2, 7] with those of the high modulus metal W[8], it is clear that the sensitive zone scale of the size effect of the former is smaller than that of the latter by a quantity level. Correspondingly, the scale of the contact radius of the former is also smaller than that of the latter by a quantity level. Furthermore, in view of the previous investigations[3, 4] whose attention was focused on the case when micro-scale was smaller than contact radius, therefore, it is necessary to discuss the case when micro-scale is larger, even several times larger than contact radius for the conventional metals (Cu, Ag, Al, etc.). In the present research, the Fleck and Hutchinson's strain gradient plasticity model[10] is used, but our attention is focused on the compressible general case. Moreover, the micro-indentation tests for single crystal copper and single crystal aluminum are carried out. The experimental programming is different from the conventional one (that is, measuring the hardness curve based on unique loading point). In the present research, we selected many loading points on the material surface randomly, and each test point corresponded to the only measured value for a hardness/depth relation. Although this method would lead to a data strip for the hardness/depth relation, it avoided the defects from the conventional unique loading point method. By comparing the theoretical prediction with the strip test data, the micro-scale parameter of strain gradient plasticity theory will be predicted.

1 Deformational theory of strain gradient plasticity

The compressible general form of the deformation theory of strain gradient plasticity has not been presented until now. However, since the projection tensor of the higher-order strains and the related operation law were presented[13], it should be easy to be derived along the frame of conventional elastic-plastic theory. A brief description is outlined as follows.

1.1 Constitutive relations

The definitions of the strain and strain gradient are dictated by

$$\varepsilon_{ij} = \frac{1}{2}(u_{i,j} + u_{j,i}) = \varepsilon^e_{ij} + \varepsilon^p_{ij}, \quad \eta_{ijk} = u_{k,ij} = \eta^e_{ijk} + \eta^p_{ijk}. \tag{1}$$

The expressions related with the constitutive relations are listed as follows:

$$W^e = E\left(\frac{\nu}{2(1+\nu)(1-2\nu)}\varepsilon^{e2}_{kk} + \frac{1}{2(1+\nu)}\varepsilon^e_{ij}\varepsilon^e_{ij} + \sum_{I=1}^{4} L^{e2}_I \eta^{e(I)}_{ijk}\eta^{e(I)}_{ijk}\right),$$

$$
\begin{aligned}
\sigma_{ij} &= \partial W^e/\partial \varepsilon^e_{ij},\ \tau_{ijk} = \partial W^e/\partial \eta^e_{ijk},\\
\Xi &= \sqrt{\frac{2}{3}\varepsilon'_{ij}\varepsilon'_{ij} + \sum_{I=1}^{3} L_I^2 \eta^{(I)}_{ijk}\eta^{(I)}_{ijk}},\\
\Sigma &= \sqrt{3J_2} = \sqrt{\frac{3}{2}\sigma'_{ij}\sigma'_{ij} + \sum_{I=1}^{3} L_I^{-2}\tau^{(I)}_{ijk}\tau^{(I)}_{ijk}},\\
\eta^{(I)}_{ijk} &= T^{(I)}_{ijklmn}\eta_{lmn},\ \tau^{(I)}_{ijk} = T^{(I)}_{ijklmn}\eta_{lmn},\\
\varepsilon^p_{ij} &= \frac{3}{2h^p}\frac{\partial J_2}{\partial \sigma_{ij}} = \frac{3}{2h^p}\sigma'_{ij},\\
\eta^p_{ijk} &= \frac{3}{2h^p}\frac{\partial J_2}{\partial \tau_{ijk}} = \frac{1}{h^p}\sum_{I=1}^{3} L_I^{-2}T^{(I)}_{ijklmn}\tau_{lmn},\\
h^p &= \Sigma/(\Xi - \Sigma/E),
\end{aligned}
\tag{2}
$$

where Σ and Ξ are the effective stress and effective strain, respectively. L^e_I and $L_I (I = 1, 4)$ are the micro-scale parameters of elastic and plastic cases, respectively. From the discussion in ref. [10], there exists a general relation among the micro-scales:

$$L_1 = L,\ L_2 = \frac{1}{2}L,\ L_3 = \sqrt{\frac{5}{24}}L. \tag{3}$$

In addition, take $L_4 = L/2$. Similarly, eq. (3) is valid also for the elasticity strain gradient case, changing L into L^e in form in eq. (3). Moreover, the previous research has shown that the solution is insensitive to the value of L^e/L within the region of $0 < L^e/L < 1$[13]. Thus, take $L^e/L = 0.5$ in the present research. In the last relation of eq. (2), h^p is the equivalent plastic modulus. Considering the strain hardening material:

$$\Xi = \Xi_0(\Sigma/\sigma_Y),\ \Sigma \leqslant \sigma_Y;\ \Xi = \Xi_0(\Sigma/\sigma_Y)^{1/N},\ \Sigma > \sigma_Y, \tag{4}$$

then, we have

$$h^p = E\{(\Sigma/\sigma_Y)^{1/N-1} - 1\}^{-1}. \tag{5}$$

In formula (2), $T^{(I)}_{ijklmn} (I = 1, 4)$ is the projection tensor of the strain gradient, and the detailed expressions have been shown in ref. [13]. Thus, by using formulas (1) and (2) and the projection tensor normality, the compressible general form of the deformational theory of strain gradient plasticity can be derived as

$$
\begin{aligned}
\sigma_{ij} &= \frac{E}{1+\nu+\frac{3}{2}E/h^p}\varepsilon_{ij} + \frac{1}{3}\left(\frac{E}{1-2\nu} - \frac{E}{1+\nu+\frac{3}{2}E/h^p}\right)\varepsilon_{kk}\,\delta_{ij},\\
\tau_{ijk} &= 2E\left\{\sum_{I=1}^{3}\frac{L_I^2}{L_I^2/L_I^{e2} + 2E/h^p}T^{(I)}_{ijklmn} + L_4^{e2}T^{(4)}_{ijklmn}\right\}\eta_{lmn}.
\end{aligned}
\tag{6}
$$

1.2 Equilibrium and variational relation

Frequently, equilibrium equations can be described by the displacement-variational relation, for the convenience of using the finite element implementation. The displacement-variational relation for the strain gradient plasticity theory is given by[10]

$$\int_V (\sigma_{ij}\delta\varepsilon_{ij} + \tau_{ijk}\delta\eta_{ijk})\mathrm{d}V = \int_V f_k\delta u_k\mathrm{d}V + \int_S t_k\delta u_k\mathrm{d}S + \int_S r_k(D\delta u_k)\mathrm{d}S. \tag{7}$$

Based on eq. (7), the traction on S surface is defined by

$$t_k = n_i\left(\sigma_{ik} - \frac{\partial \tau_{ijk}}{\partial x_j}\right) + n_i n_j \tau_{ijk}(D_p n_p) - D_j(n_i \tau_{ijk}), \tag{8}$$

and a surface torque by $r_k = n_i n_j t_{ijk}$. The operators D and D_j in eqs. (7) and (8) are defined as

$$D_j = \partial/\partial x_j - n_j n_k \partial/\partial x_k, \quad D = n_k \partial/x_k, \tag{9}$$

where n_i in eqs. (7)—(9) is the direction cosine on S surface.

2 Fundamental mechanics in the micro-indentation test

Consider that the pressure head is a circular cone. Pyramid pressure head can be replaced approximately with circular cone according to the cross-section area equivalence. A traction condition on the remote boundary is used here, instead of the displacement boundary conditions as usually did. Such a treatment is not only close to the true status for indentation test, but also greatly simplifies the description and analysis.

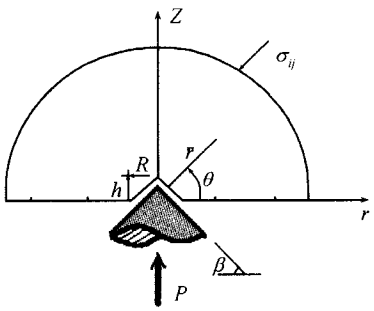

Fig. 1. Mechanics description for indentation test.

Elastic stress distributions on the remote boundary have been given as (see fig. 1 for reference)[14]

$$\sigma_r = \frac{P}{2\pi\bar{r}^2}\left\{\frac{1-2v}{1+\sin\theta} - 3\cos^2\theta\sin\theta\right\}, \quad \sigma_z = -\frac{3P}{2\pi\bar{r}^2}\sin^3\theta,$$
$$\sigma_{rz} = -\frac{3P}{2\pi\bar{r}^2}\cos\theta\sin^2\theta, \quad \sigma_\varphi = \frac{(1-2v)P}{2\pi\bar{r}^2}\left\{\sin\theta - \frac{1}{1+\sin\theta}\right\}, \tag{10}$$

where $\bar{r}^2 = r^2 + z^2$. The definitions of the others are shown in fig. 1.

The mixed boundary conditions on the material surface ($z = 0$) in a small deformation case are imposed by

$$u_z = -r\tan\beta, \quad R_r = 0, \quad R_z \leqslant 0, \quad 0 \leqslant r \leqslant R = h/\tan\beta,$$
$$R_r = R_z = 0, \quad R \leqslant r, \tag{11}$$

where the reference point of vertical displacement u_z is defined at the conical apex; R is the contact radius; h is penetration depth of indenter; R_r and R_z are surface traction.

For the convenience of the analysis, define a length parameter as

$$R_0 = \sqrt{P/(3\pi\sigma_Y)}. \tag{12}$$

R_0 is the conventional contact radius (no size effect) for the low-hardening metal material in the case of flat pressure head[15]. The hardness definition and the relations with geometrical parameter and indent depth are given by

$$H = \frac{P}{\pi R^2} = 3\sigma_Y\left(\frac{R_0}{R}\right)^2 = 3\sigma_Y\left(\frac{R_0}{h}\tan\beta\right)^2. \tag{13}$$

In all relations given above, any parameters or variables with length dimension can be normalized by R_0, and any quantities with stress dimension can be normalized by σ_Y, such that the normalized hardness can be taken to be a function of the independent and nondimensional parameters as follows:

$$\frac{H}{\sigma_Y} = f\left(\frac{E}{\sigma_Y}, \nu, N, \beta, \frac{L}{R_0}\right), \tag{14}$$

while contact radius and indent depth are related to the hardness by eq. (13). The detailed expression of eq. (14) will be implemented by solving the indentation problem numerically, using

the strain gradient plasticity theory.

3 Finite element method for the deformational theory of strain gradient plasticity

For the constitutive relation considering strain gradient effect, generally speaking, the conventional finite element method fails to be used, and a special finite element method taking the displacement derivatives as the nodal variables is needed[13, 16, 17]. However, for the stretching-dominated strain gradient plasticity problem, one can obtain an effective result by adopting the iso-parametric displacement element with nine nodes[13, 17]. Obviously, the indentation problem is stretching-dominated. Therefore, in the present analysis, such an element will be used. In addition, 2×2 Gauss integration points are adopted for each element.

For the axisymmetrical problem of indentation test, considering that the elastic stress field acts on the remote boundary, the pressure head apex is taken as the reference point (zero point) of vertical displacement. Thus, imagining that under the action of remote stress field, material would move back to the pressure head surface; near the apex, material would contact with conical surface, and the contact radius would be equal to R. The displacement constraint conditions in contact region are described by eq. (11).

Using the plastic deformational theory, the solution procedures can be outlined as follows: First, calculate the elastic solution; second, taking the elastic solution as the initial trial, find the solution for the higher-hardening material by iterating; and third, taking the last solution as the new initial trial, find the convergent solution for the lower-hardening material case by iterating. For example, the solution procedures for $N = 0.1$ case are described as follows: First, find the elastic solution and then take it as the initial solution calculate the convergent solution for $N = 0.3$ case by iterating; second, taking the last solution ($N = 0.3$) as a new initial trial, find the convergent solution for the case of $N = 0.2$ by iterating; finally, based on the solution of $N = 0.2$, find the convergent solution for $N = 0.1$ by iterating.

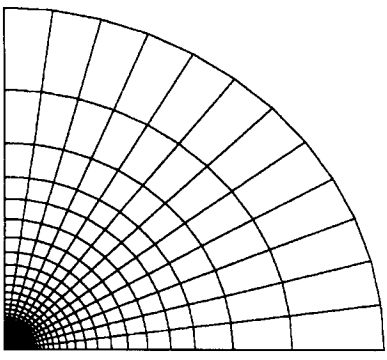

Fig. 2. Finite element mesh for axisymmetric problem.

Considering the true case for micro-indentation test problem, take the remote boundary as the reference point of vertical displacement. Thus, the vertical displacement field can be converted by

$$v(r, z) = u_z(r, z) - u_z^{\infty}, \tag{15}$$

where u_z^{∞} is the vertical displacement at the remote boundary in the case when conical apex is defined the reference point of vertical displacement.

The form of finite element mesh adopted in the present research is shown in fig. 2. The number of the nine nodal elements used in the calculation is 1280.

4 Numerical results and analysis

In the analysis of the conventional metal materials, take material parameters as (E/σ_Y, ν, N) = (300, 0.3, 0.1) and consider the flat pressure head case. First, investigate the pile-up and sink-in phenomena, then predict the relations between the hardness and the indent depth for the material parameters (see eq. (14)). Note that the conventional flat pyramid cone pressure

head is equivalently replaced by the flat circular conical head for the convenience of analysis, and the equivalent conical angle β is about 20—30 degrees. Therefore, in the present research, take the pressure head angles as $\beta = 30°$.

Fig. 3(a) and (b) illustrate the radial and vertical displacements on the material surface ($z = 0$). Comparing the two kinds of displacements, the vertical displacement is far greater than the radial displacement within the contact region. From fig. 3(b), we can see that near the outer boundary of the contact region, the material is piled up. With increasing the micro-scale parameter, the pile-up phenomenon is gradually weakened and transferred to the sink-in phenomenon.

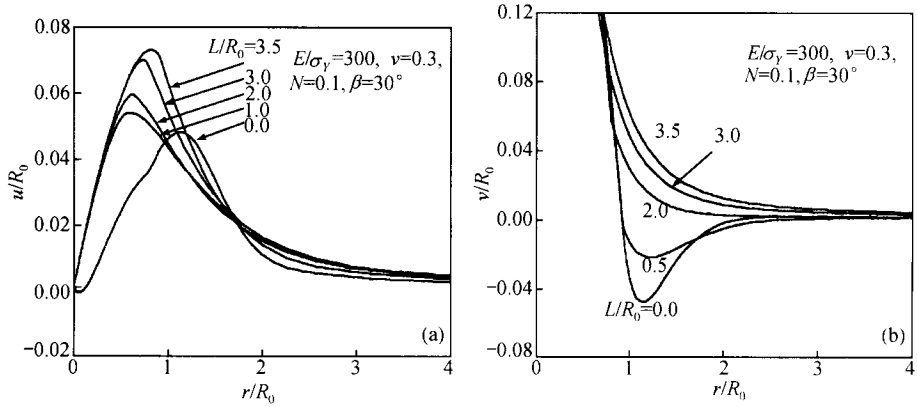

Fig. 3. The displacement distributions on the material surface. (a) Radial displacements; (b) vertical displacements.

The variations of vertical displacement against material yielding strain (σ_Y/E) are shown in fig. 4 when the strain gradient effect is neglected. From fig. 4, we find that the lower the material yielding strain (the smaller elastic deformation), the easier the pile-up phenomenon taking place. With increasing the yielding strain, the pile-up phenomenon on the material surface is gradually transferred to the sink-in phenomenon. The transition point of yielding strain from the pile-up to the sink-in is about 1/70 when strain gradient effect is neglected. This result is consistent with that given in ref. [9] for elastic perfectly plastic material.

In fig. 5, the variations of hardness with the indent depth for several strain-hardening exponential materials are shown, where R_0/L has been converted into h/L from eq. (13). For lower-hardening materials (conventional flexible metal materials), when the ratio of the indent depth to the micro-scale parameter decreases and falls down to the region of 0.1— 0.3, the size effect increases sharply. Inversely, when the ratio is larger than 0.6, the size effect is insensitive. For the higher-hardening materials, such as $N = 0.2$ or 0.3, the sensitive region of size effect is relatively large. For comparison, the curve of hardness against indent depth for the conventional metal materials obtained from the dislocation model[1] is also shown in fig. 5. From fig. 5, with increasing the indent depth further, especially when the ratio h/L is greater than 1, the material hardness tends to triple the yielding stress. This value is just the conventional hardness for weak-hardening materials and for the flat conical pressure head case, when strain gradient effect is neglected[17].

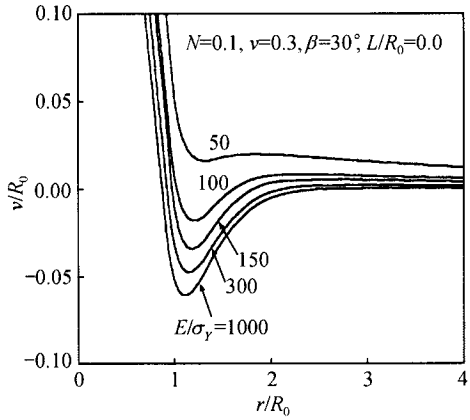

Fig. 4. Vertical displacement distributions on material surface for several yielding strain materials.

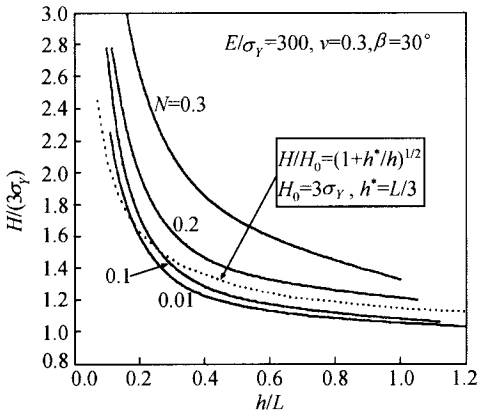

Fig. 5. Variations of hardness with indent depth for several strain-hardening materials.

5 Micro-indentation tests for single crystal Cu and Al and the micro-scale prediction

The detailed experimental researches are carried out for the single crystal copper and the single crystal aluminum (both along the (110) surface) at the National Key Laboratory of Friction and Lubrication, Tsinghua University; and the National Key Laboratory of Nonlinear Mechanics, Institute of Mechanics, Chinese Academy of Sciences.

Conventional experimental results of the indentation hardness are measured based on a unique loading point on the material surface. The experimental curve of hardness vs depth is relatively smooth. However, such a hardness curve should be dependent on the status at the loading point (defects or reinforced particles, etc.). In view of the reasons, in the present experimental research, we select many loading points and indent depths on the surface, and one loading point corresponds to the only one measured value for the hardness/depth relation, so that a data strip about the hardness/depth relation is obtained. Furthermore, based on the data strip, a region of the micro-scale parameter can be determined.

In fig. 6, the scanning electronic photographs of three depth indents and the material surface profile for the single crystal copper are shown. The pile-up phenomenon near the outer boundary of indents takes place from the figure, seeing the bright region (piling up) around the outer boundary of indents. The pile-up phenomenon is obvious in fig. 6(b).

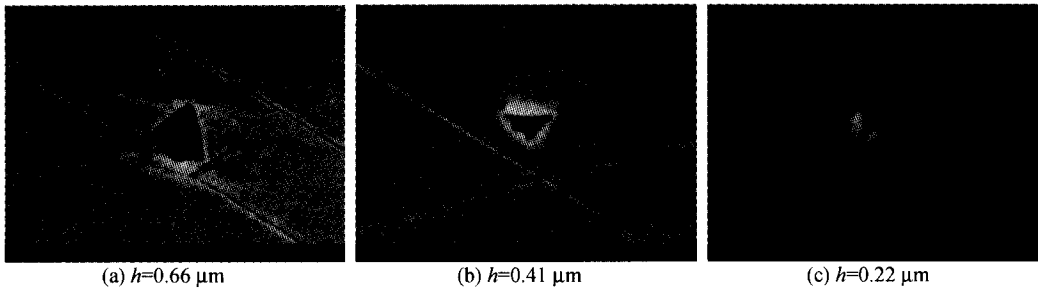

(a) h=0.66 μm (b) h=0.41 μm (c) h=0.22 μm

Fig. 6. SE photographs of three indent depths and surface profile for single crystal Cu.

Experimental results of the hardness/depth relation for single crystal copper are given in fig. 7. Meanwhile, the prediction results ($N = 0.1$) corresponding to those shown in fig. 5 are also

superimposed in fig. 7 for comparison. When the micro-scale is taken as 0.5 and 1.5 μm, respectively, nearly all experimental data for the single crystal copper are covered. The prediction results characterize the size effect of the material fairly.

The experimental results and the simulation results of the hardness/depth relation by using the strain gradient plasticity theory for the single crystal aluminum are shown in fig. 8. When the micro-scale parameter is taken as 1 and 2 μm, respectively, nearly all experimental data are covered.

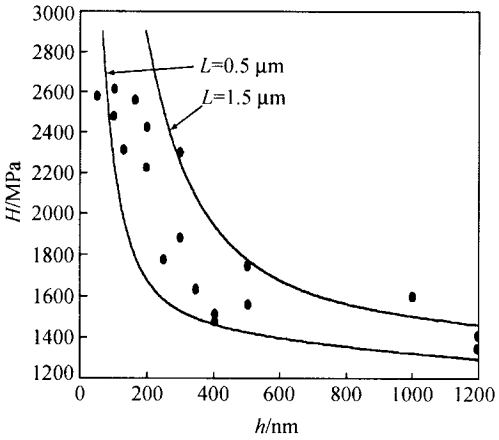

Fig. 7. Experimental results and prediction results of the hardness/depth relation for single crystal Cu. ●, Single crystal Cu(110).

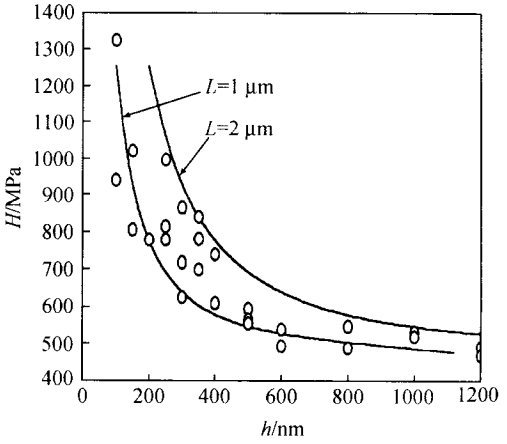

Fig. 8. Experimental results and prediction results of the hardness/depth relation for single crystal Al. ○, Single crystal Al(110).

In order to further assess the effectiveness of the strain gradient plasticity theory in accounting for the size effect of indentation tests, the experimental results for the single crystal and polycrystalline Cu given by McElhaney et al.[2] and for single crystal Ag given by Ma et al.[7], and for comparison the present prediction results, are shown in figs. 9 and 10, respectively. Similarly, it is clear that the size effect of the micro-indentation tests can be caught effectively by using the strain gradient plasticity theory.

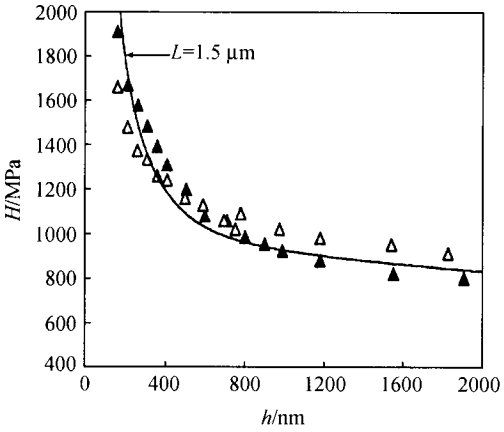

Fig. 9. Experimental results[2] and present prediction results of the hardness/depth relation for single crystal and polycrystalline Cu. △, Cold worked polycrystalline Cu; ▲, single crystal Cu(111).

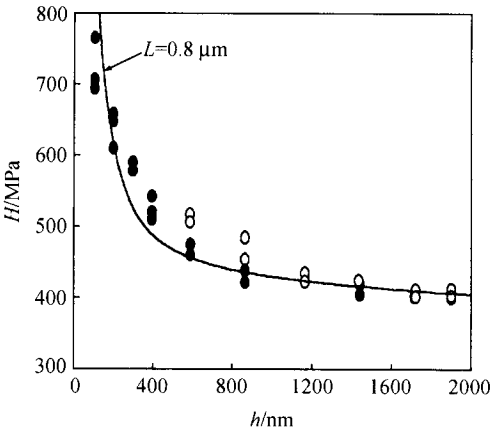

Fig. 10. Experimental results[7] and present prediction results of the hardness/depth relation for single crystal Ag. ●, Single crystal Ag(110); ○, single crystal Ag(100).

6 Conclusions

In the present research, the size effects of the micro-indentation tests have been simulated and predicted by using the finite element implementation based on the strain gradient plasticity theory, meanwhile, the experimental researches of the micro-indentation tests for single crystal copper and single crystal aluminum have been carried out. Through the theoretical research and experimental research, the main conclusions have been obtained as follows:

(i) For conventional metal materials, the pile-up phenomenon near the contact zone boundary predicted from the conventional elastic-plastic theory will take place extensively. However, the pile-up phenomenon predicted from strain gradient plasticity theory will be weak, or will never take place and be transferred to the sink-in phenomenon. Moreover, the pile-up and sink-in phenomena are closely dependent of the yielding strain of material. The material with the low yielding strain is favorable for the pile-up phenomenon, while the material with the high yielding strain is favorable for the sink-in phenomenon.

(ii) For the indentation tests of the conventional metal materials, the sensitive region of the size effect is situated when indent depth is smaller than the material micro-scale; especially, when indent depth is smaller than 1/3 of the micro-scale, the size effect is very sensitive. Inversely, when indent depth is greater than the micro-scale parameter, the size effect is very weak, such that the conventional elastic-plastic theory can be used to describe the indentation tests.

(iii) For the conventional metal materials, the values of the micro-scale parameter in the strain gradient plasticity theory will be taken within the region of 0.8—1.5 μm.

Acknowledgements This work was supported by the National Natural Science Foundation of China (Grant Nos. 19891180 and 19925211), and jointly supported by the Fundamental Research Project from the Chinese Academy of Sciences (Grant No. KJ95-1-201).

References

1. Nix, W. D., Gao, H., Indentation size effects in crystalline materials: a law for strain gradient plasticity, J. Mech. Phys. Solids, 1998, 46(3): 411.
2. McElhaney, K. W., Vlassak, J. J., Nix, W. D., Determination of indenter tip geometry and indentation contact area for depth-sensing indentation experiments, J. Mater. Res., 1998, 13(5): 1300.
3. Begley, M., Hutchinson, J. W., The mechanics of size-dependent indentation, J. Mech. Phys. Solids, 1998, 46: 1029.
4. Shu, J. Y., Fleck, N. A., The prediction of a size effect in micro-indentation, Int. J. Solids Structures, 1998, 35(13): 1363.
5. Poole, W. J., Ashby, M. F., Fleck, N. A., Micro-hardness tests on annealed and work-hardened copper polycrystals, Scripta Metall Mater, 1996, 34: 559.
6. Atkinson, M., Further analysis of the size effective in indentation hardness tests of some metals, J. Mater. Res., 1995, 10: 2908.
7. Ma, Q., Clarke, D. R., Size dependent hardness of silver single crystals, J. Mater. Res., 1995, 10: 853.
8. Stelmashenko, N. A., Walls, M. G., Brown, L. M. et al., Microindentation on W and Mo priented single crystals: an STM study, Acta Metall Mater, 1993, 41: 2855.
9. Cheng, Y. T., Cheng, C. M., Scaling relationships in conical indentation of elastic-perfectly plastic solids, Int. J. Solids Structures, 1999, 36: 1231.
10. Fleck, N. A., Hutchinson, J. W., Strain gradient plasticity, in Advances in Applied Mechanics (eds. Hutchinson, J. W., Wu, T. Y.), 1997, 33: 295.
11. Gao, H., Huang, Y., Nix, W. D. et al., Mechanism-based strain gradient plasticity — I, Theory. J Mech Phys Solids, 1999, 47: 1239.
12. Aifantis, E. C., On the microstructural origin of certain inelastic models, Trans. ASME J. Eng. Mater. Tech., 1984, 106: 326.
13. Wei, Y., Hutchinson, J. W., Steady-state crack growth and work of fracture for solids characterized by strain gradient plasticity, J. Mech. Phys. Solids, 1997, 45(8): 1253.
14. Timoshenko, S. P., Goodier, J. N., Theory of Elasticity, 3rd ed., New York: McGraw-Hill, Inc., 1970, 401.
15. Shaw, M. C., In Mechanical Behavior of Materials (eds. McClintock, F. A., Argon, A. S.), Reading: Addison-Wesley, 1966, 443.
16. Xia, Z. C., Hutchinson, J. W., Crack tip fields in strain gradient plasticity, J. Mech. Phys. Solids, 1996, 44: 1621.
17. Chen, J. Y., Wei, Y., Huang, Y. et al., The crack tip fields in strain gradient plasticity: the asymptotic and numerical analyses, Eng. Fract. Mech., 1999, 64: 625.